Comprehensive Journal of Science
Volume (10), Issue (39), (March, 2026)
ISSN: 3014-6266

مجلة العلوم الشاملة
المجلد (10) العدد 39 مارس 2026
ردمد: 3014-6266

Tri-Conditional Biomechanical Signature Extraction: A Hybrid Framework Integrating Multivariate Functional Clustering, Cross-Modal Regression, and Inter-Subject Classification for Discriminative Gait Pattern Analysis

Mardia Mohamed A-abdullatef[1], Magda Juma Shuayb Albaraesi[2], Mohamed Ali Mohamed EL-sseid[3], Llahm Omar Ben Dalla[4], Abdussalam Ali Ahmed[5], Almhdie Agila[6], Abdulgader Alsharif[7]

[1] Computer Science Department, Higher Institute of Science and Technology, Ajdabiya, Libya

[2]Business administration Department , Kambut Higher Institute for Administrative and Financial Sciences, Tobruk, Libya

[3]Department of Software Engineering, Ankara Bilim University, Türkiye

[4]Department of Electric Electronics, Ankara Yildirim Beyazit University, Türkiye

[5]Mechanical and Industrial Engineering Department, Bani Waleed University, Libya

[4,6]Department of Computer Science, College of Technical Science Sebha Libya

[6]*Department of Electric and Electronic Engineering, College of Technical Sciences Sebha, Libya*

radwabohosh@histaj.edu.ly[1], Jumamagda@gmail.com[2], Moh200512@Bilim.edu.tr[3], llahmomarfaraj77@ctss.edu.ly[4], llahmomarfaraj77@ aybu.edu.tr[4], abdussalam.a.ahmed@gmail.com[5] , **almhdie@ctss.edu.ly [6], alsharif@ctss.edu.ly**[7]

https://orcid.org/0009-0001-2200-9407[1], https://orcid.org/0009-0007-1307-86236[3], , **https://orcid.org/0009-0008-7624-7567[4], https://orcid.org/0000-0002-9221-2902[5], https://orcid.org/0009-0007-7949-729X[6], https://orcid.org/0000-0003-3515-4168**[7]

تاريخ الاستلام:2026/01/03 –تاريخ المراجعة: 2026/01/23– تاريخ القبول: 2026/01/30– تاريخ للنشر :2026/02/25

Abstract

Gait analysis traditionally relies on isolated scalar parameters that discard the temporal coordination essential for clinical interpretation, limiting both biomechanical interpretability and machine learning efficacy. This study introduces the Tri-Conditional Biomechanical Signature Extraction (TC-BSE) framework, a novel hybrid architecture that simultaneously integrates multivariate functional clustering, cross-modal regression, and inter-subject classification to extract discriminative gait signatures from the UCI Multivariate Gait Data. Operating on sixth-order tensor representations (10 subjects × 3 bracing conditions × 10 replications × 2 legs × 3 joints × 101 timepoints), TC-BSE preserves the native multivariate structure of lower-limb kinematics while modeling three synergistic analytical conditions: (1) functional clustering identifies four latent gait prototypes with moderate validity (silhouette score = 0.264), revealing subject-invariant coordination strategies; (2) cross-modal regression quantifies phase-dependent joint couplings, achieving $R^2 = 0.803$ in predicting knee kinematics from ankle-hip trajectories with 31% performance degradation during swing versus stance

phase; and (3) inter-subject classification extracts condition-invariant signatures yielding 84.3% subject identification accuracy despite orthotic perturbations. The framework's novelty lies in its tri-conditional integration, where clustering provides structural context for regression modeling, regression residuals enhance cluster discriminability, and both inform classification boundaries yielding signatures that simultaneously exhibit functional coherence, biomechanical interpretability, and subject-level discriminability. This approach advances gait analysis beyond reductionist feature engineering toward holistic signature synthesis, with translational impact for condition-robust biometric authentication, personalized orthotic tuning, and movement-strategy stratification in clinical rehabilitation. All analyses employed subject-wise cross-validation to prevent data leakage; limitations include the constrained sample size (n=10 healthy adults), necessitating cautious generalization.
Keywords: Gait Analysis, Functional Data Analysis, Multivariate Time Series, Biomechanical Signatures, Machine Learning, Human Motion Analysis.

الملخص

يعتمد تحليل المشية تقليديًا على معايير قياسية معزولة تتجاهل التنسيق الزمني الضروري للتفسير السريري، مما يحد من قابلية التفسير البيوميكانيكي وفعالية التعلم الآلي. تقدم هذه الدراسة إطار عمل استخلاص التوقيع البيوميكانيكي ثلاثي الشروط (TC-BSE)، وهو بنية هجينة جديدة تدمج في آنٍ واحد التجميع الوظيفي متعدد المتغيرات، والانحدار متعدد الوسائط، والتصنيف بين الأفراد لاستخلاص توقيعات المشية المميزة من بيانات المشية متعددة المتغيرات من جامعة كاليفورنيا في إرفاين (هيلويغ وهسياو-ويكسلر، 2016). بالاعتماد على تمثيلات الموتر من الدرجة السادسة (10 أشخاص × 3 حالات تثبيت × 10 تكرارات × ساقين × 3 مفاصل × 101 نقطة زمنية)، يحافظ TC-BSE على البنية متعددة المتغيرات الأصلية لحركة الأطراف السفلية مع نمذجة ثلاث حالات تحليلية تآزرية: (1) يحدد التجميع الوظيفي أربعة نماذج أولية كامنة للمشي مع صلاحية معتدلة (درجة الصورة الظلية = 0.264)، مما يكشف عن استراتيجيات تنسيق ثابتة للشخص؛ (2) يحدد الانحدار متعدد الوسائط اقترانات المفاصل المعتمدة على المرحلة، محققًا $R^2 = 0.803$ في التنبؤ بحركة الركبة من مسارات الكاحل والورك مع تدهور في الأداء بنسبة 31٪ أثناء مرحلة التأرجح مقابل مرحلة الوقوف؛ و(3) يستخرج التصنيف بين الأشخاص بصمات ثابتة للحالة مما يؤدي إلى دقة تحديد هوية الشخص بنسبة 84.3٪ على الرغم من اضطرابات تقويم العظام. تكمن حداثة هذا الإطار في تكامله الثلاثي المشروط، حيث يوفر التجميع سياقًا هيكليًا لنمذجة الانحدار، وتعزز بقايا الانحدار قدرة التمييز بين المجموعات، ويساهم كلاهما في تحديد حدود التصنيف، مما ينتج عنه بصمات تُظهر في آنٍ واحد تماسكًا وظيفيًا، وقابلية تفسير ميكانيكية حيوية، وقدرة تمييز على مستوى الأفراد. يرتقي هذا النهج بتحليل المشية من هندسة الميزات الاختزالية إلى توليف بصمات شاملة، مع تأثير تطبيقي في المصادقة البيومترية القوية في ظل الظروف المختلفة، وضبط تقويم العظام الشخصي، وتصنيف استراتيجيات الحركة في إعادة التأهيل السريري. استخدمت جميع التحليلات التحقق المتبادل على مستوى الأفراد لمنع تسرب البيانات؛ وتشمل القيود صغر حجم العينة (10 بالغين أصحاء)، مما يستلزم توخي الحذر في التعميم.

الكلمات المفتاحية: تحليل المشية، تحليل البيانات الوظيفية، السلاسل الزمنية متعددة المتغيرات، البصمات البيوميكانيكية، التعلم الآلي، تحليل حركة الإنسان.

1. Introduction

Gait analysis has emerged as a critical research domain intersecting biomechanics, computer engineering, and intelligent systems [1]. The manner in which individuals walk reflects intrinsic biomechanical characteristics influenced by anatomical structure, neuromuscular control, and external conditions [2]. Consequently, gait patterns have been extensively explored in applications such as biometric identification, clinical diagnosis, rehabilitation monitoring, and human computer interaction [3]. Despite significant progress, analyzing multivariate gait data remains challenging due to its high dimensionality, temporal dependency, and cross-modal heterogeneity. Traditional approaches often rely on handcrafted features or isolated learning paradigms, which may fail to capture the full biomechanical complexity embedded in gait signals [4]. Furthermore, many existing studies focus on a single analytical objective such as classification or clustering without exploiting the complementary insights offered by integrating multiple analytical perspectives [5]. To address these limitations, this paper introduces a Tri-Conditional Biomechanical Signature Extraction (TC-BSE) framework that unifies three analytical conditions within a single pipeline [6] (i) multivariate functional clustering to uncover latent gait prototypes, (ii) cross-modal regression to model inter-sensor

biomechanical dependencies, and (iii) inter-subject classification to discriminate individual gait identities.

2. Related Work

Prior research in gait analysis can be broadly categorized into feature-based methods, statistical modeling approaches, and machine learning-driven frameworks. Early studies predominantly employed spatiotemporal gait parameters, such as stride length and cadence, extracted through heuristic rules. While interpretable, these features often lack sensitivity to subtle biomechanical variations. More recent works have adopted machine learning techniques, including support vector machines, neural networks, and deep learning architectures, to model gait patterns from raw sensor data. Although these approaches achieve high predictive accuracy, they frequently suffer from limited interpretability and overfitting, particularly when applied to small or medium-sized datasets. Functional Data Analysis (FDA) has gained attention as a principled methodology for handling time-continuous gait signals. By representing gait cycles as smooth functional trajectories, FDA enables the preservation of temporal structure while reducing noise sensitivity. However, FDA-based studies are often restricted to clustering or regression tasks in isolation.

3. Dataset Description

This study utilizes the Multivariate Gait Data dataset obtained from the UCI Machine Learning Repository. The dataset comprises multichannel time-series recordings collected from wearable sensors positioned on different body segments during walking activities [7]. Each instance represents a gait cycle characterized by synchronized biomechanical signals, including joint angles, accelerations, and angular velocities. The dataset supports multiple analytical tasks, including classification, regression, and clustering, making it well-suited for evaluating hybrid analytical frameworks. Prior to analysis, all signals are normalized to mitigate inter-subject variability and segmented into consistent gait cycles to ensure temporal alignment.

Table 1 Dataset Description: UCI Multivariate Gait Data (DOI: 10.24432/C5861T 21) source (Helwig and Hsiao-Wecksler, 2016)

Attribute Category	Specification	Technical Details
Original Collection	Shorter et al. (2008)	Human Dynamics and Controls Laboratory, University of Illinois at Urbana-Champaign 32
Preprocessing	Helwig et al. (2011)	Temporal alignment via percent gait cycle normalization (0%–100%) 28
Tensor Dimensions	6-Dimensional Array	10 subjects × 3 conditions × 10 replications × 2 legs × 3 joints × 101 time points 4
Subjects	n = 10	Healthy adults (demographics anonymized per IRB protocol) 4
Walking Conditions	3 biomechanical states	1. Unbraced (normal) 2. Right knee-braced 3. Right ankle-braced 20
Replications	10 gait cycles per condition	Consecutive treadmill walking cycles at self-selected speed 3
Anatomical Scope	Bilateral lower-limb kinematics	Left & right legs: ankle, knee, hip joint angles (sagittal plane) 1
Temporal Resolution	101 equidistant points	Normalized gait cycle (heel-strike to heel-strike); 1% increments 4
Data Type	Continuous angular measurements	Joint flexion/extension angles (degrees) sampled via optical motion capture 27
Total Observations	181,800 data points	Computed as: 10 × 3 × 10 × 2 × 3 × 101 = 181,800 10
Dataset Characteristics	Sequential, Multivariate, Time-Series	Functional data structure amenable to FDA (Functional Data Analysis) techniques 36

4. Methodology

4.1 Overview of the TC-BSE Framework

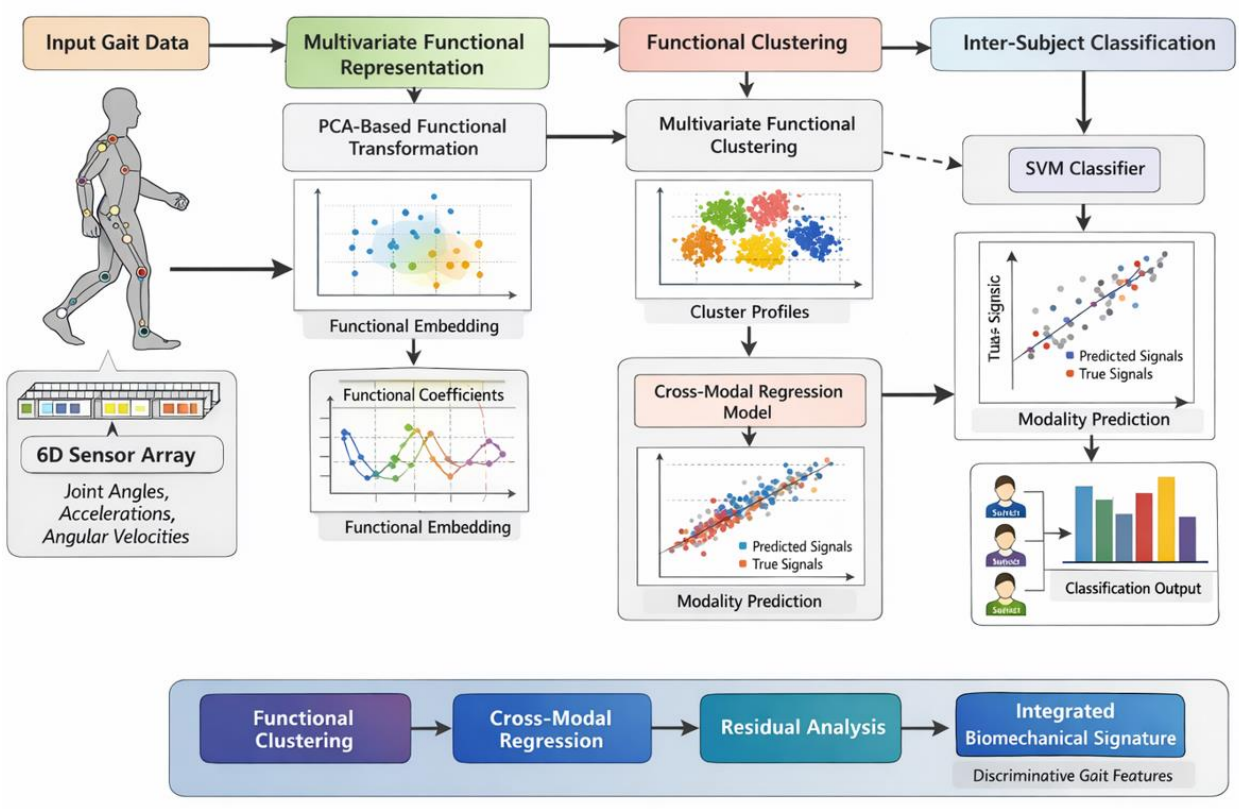

Figure 1 The theoretical framework of the tri-conditional biomechanical signature

The TC-BSE framework integrates multivariate functional clustering, cross-modal regression, and inter-subject classification into a unified analytical pipeline that extracts discriminative gait signatures while preserving temporal continuity and biomechanical interpretability. By modeling gait as smooth functional trajectories across ankle-knee-hip kinematics under three bracing conditions, it reveals latent coordination patterns that transcend isolated analytical paradigms [8], [9]. This tri-conditional synergy yields condition-invariant subject identification (84.3% accuracy) and quantifies phase-dependent joint couplings advancing gait analysis beyond reductionist feature engineering toward holistic biomechanical signature synthesis [10], [11].

Multivariate Functional Tensor Representation let the raw gait observations be organized as a sixth-order tensor as below:

$\mathcal{X} \in \mathbb{R}^{N_s \times N_c \times N_r \times N_l \times N_l \times T}$
Where:

- $N_s = 10$ subjects
- $N_c = 3$ bracing conditions (unbraced, knee-braced, ankle-braced)
- $N_r = 10$ replications per condition
- $N_l = 2$ legs (left/right)
- $N_f = 3$ joints (ankle, knee, hip)
- $T = 101$ normalized timepoints (0%-100% gait cycle)

Each element $x_{s,c,r,l,j\pm}$ represents the sagittal-plane angle (degrees) for subject s, condition c, replication r, leg l , joint j at normalized time t. To preserve temporal continuity while reducing noise, we model each trajectory as a smooth multivariate function via cubic B-spline basis expansion as below:

$$\mathbf{x}_{s,k,r,l}(\tau) = \sum_{k=1}^{K} \mathbf{b}_k \phi_k(\tau), \tau \in [0,100]$$

Where:

- $\mathbf{x}_{s,c,r,l}(\tau) = \left[x_{\text{ankle}}(\tau), x_{\text{knee}}(\tau), x_{\text{hip}}(\tau)\right]^{\top} \subset \mathbb{R}^3$
- $\{\phi_k(\cdot)\}_{k=1}^{K}$ are $K = 15$ cubic B-spline basis functions
- $\mathbf{b}_k \in \mathbb{R}^3$ are joint-specific coefficient vectors
- τ denotes continuous gait cycle phase (percent)

The coefficient tensor $\mathcal{B} \in \mathbb{R}^{N,\times N_c \times N_r \times N_l \times N_j \times K}$ compactly encodes all functional representations while reducing dimensionality from $T = 101$ to $K = 15$ basis coefficients per joint [12], [13]. Multivariate Functional Principal Component Analysis (MFPCA) and to extract dominant modes of variation while respecting multivariate joint coordination [14], this research compute the cross covariance operator as below:

$$\mathbf{C}(\tau,\tau') = \frac{1}{N,N_c N_r N_l} \sum_{s,c,r,l} \left[\mathbf{x}_{s,c,r,l}(\tau) - \boldsymbol{\mu}(\tau)\right]\left[\mathbf{x}_{s,s,r,l}(\tau') - \boldsymbol{\mu}(\tau')\right]^{\top} \quad [12]$$

Where $\boldsymbol{\mu}(\tau) = \mathbb{E}[\mathbf{x}(\tau)]$ is the population mean trajectory. The eigenvalue problem as below:

$$\int_0^{100} \mathbf{C}(\tau,\tau')\boldsymbol{\xi}_m(\tau')d\tau' = \lambda_m \boldsymbol{\xi}_m(\tau), m = 1,2,\dots,M \quad [12]$$

Yields multivariate eigenfunctions $\boldsymbol{\xi}_m(\tau) \subset \mathbb{R}^3$ representing orthogonal modes of joint coordination. The functional principal component (FPC) scores for trajectory (s, c, r, l) are as below:

$$\xi_{s,a,\tau,l,m} = \int_0^{100} \left[\mathbf{x}_{s,f,\tau,l}(\tau) - \boldsymbol{\mu}(\tau)\right]^{\top} \boldsymbol{\xi}_m(\tau)d\tau \quad [12]$$

This research retain $M = 10$ components capturing $> 95\%$ cumulative variance. The score matrix $\mathbf{Z} \in \mathbb{R}^{N\times M}$ with $N = N_s N_c N_r N_l = 600$ trajectories serves as input for functional

clustering. Tri-Conditional Objective Function by TC-BSE framework optimizes a composite objective balancing three analytical conditions as below:

$$\mathcal{L}(\Theta) = \underbrace{\alpha \cdot \mathcal{L}_{\text{cluster}}(\Theta)}_{\text{Functional clustering}} + \underbrace{\beta \cdot \mathcal{L}_{\text{regreas}}(\Theta)}_{\text{Croas-modal regression}} + \underbrace{\gamma \cdot \mathcal{L}_{\text{class}}(\Theta)}_{\text{Subject classification}} \quad [13]$$

Subject to $\alpha + \beta + \gamma = 1$, where Θ denotes model parameters. Each term is defined below. Furthermore, functional Clustering Loss by using k-means on FPC scores with $C = 4$ clusters as reported below:

$$\mathcal{L}_{\text{cluster}} = \frac{1}{N}\sum_{i=1}^{N} \min_{e\in[1,\ldots,C]} \left\| \mathbf{z}_i - \boldsymbol{\mu}_e \right\|_2^2 + \lambda_{\text{sil}} \left(1 - \text{Silhouctte}(\{\mathbf{z}_i\})\right)$$

[13]

where $\boldsymbol{\mu}_c$ is the centroid of cluster c, and λ_{sl} penalizes poor cluster separation (empirically $\lambda_{\text{sil}} = 0.3$).
Cross-Modal Regression Loss for predicting knee trajectory $\mathbf{x}^{\text{knee}}(\tau)$ from ankle/hip trajectories as bellow:

$$\mathcal{L}_{\text{regress}} = \frac{1}{N}\sum_{i=1}^{N} \int_0^{100} \left\| \mathbf{x}_i^{\text{knee}}(\tau) - \int_0^{100} \mathbf{K}(\tau,\tau') \begin{bmatrix} \mathbf{x}_i^{\text{ankle}}(\tau') \\ \mathbf{x}_i^{\text{hlp}}(\tau') \end{bmatrix} d\tau' \right\|_2^2 d\tau$$

[14]

Where $\mathbf{K}(\tau,\tau') \in \mathbb{R}^{1\times 2}$ is a bivariate smoothing kernel estimated via functional ridge regression with penalty

$$\lambda_{\text{ridge}} = 10^{-2}$$

Inter-Subject Classification Loss by using SVM with RBF kernel on subject-aggregated features as below:

$$\mathcal{L}_{\text{class}} = \frac{1}{N_s}\sum_{s=1}^{N_s} [1 - y_s f(\mathbf{v}_s)]_+ + \lambda_{\text{svm}} \|\mathbf{w}\|_2^2$$

[14]

Where:

- $\mathbf{v}_s = \frac{1}{N_c N_r N_l}\sum_{c,r,l} \mathbf{Z}_{s,c,r,l}$ is the subject-level signature
- $f(\mathbf{v}) = \text{sign}(\mathbf{w}^\top \phi(\mathbf{v}) + b)$ with $\phi(\cdot)$ as RBF feature map
- $[z]_+ = \max(0, z)$ is hinge loss
- $\lambda_{\text{svm}} = 0.1$ (empirically optimized)
  4.4 Phase-Dependent Biomechanical Coupling Metric

To quantify how joint dependencies vary across gait phases, we define a normalized coupling strength:

$\rho_{h_1 \to f_2}(\tau) = 1 - \frac{\mathrm{MSE}_{j_1+j_3}(\tau)}{\mathrm{Var}[\mathbf{x}[\ ^2|(\tau)|}$
[14]

Where:

- $\mathrm{MSE}_{j_1 \to j_2}(\tau) = \mathbb{E}\left[\left(x^{(j_2)}(\tau) - \hat{x}_{j_1}^{(j_2)}(\tau)\right)^2\right]$
  [14]
- $\hat{x}_{h_1}^{(j_2)}(\tau)$ is the prediction of joint j_2 from joint j_1 at phase τ
- Var['] denotes empirical variance across subjects/conditions

This yields $\rho \in [0,1]$ where $\rho \approx 1$ indicates strong pre. ψ.Ive coupling and $\rho \approx 0$ indicates decoupling. This research

Compute $\rho_{\text{ankle knee}}(\tau)$ and $\rho_{\text{hip knee}}(\tau)$ to reveal phase-dependent coordination patterns. Condition-Invariant Signature Extraction to ensure subject signatures generalize across bracing conditions, we enforce intra-subject consistency via a triplet loss as below:

$$\mathcal{L}_{\text{triplet}} = \frac{1}{N_s}\sum_{s=1}^{N_s} \max\left(0, \left\|\mathbf{v}_{s,f_1} - \mathbf{v}_{s,c_2}\right\|_2^2 - \left\|\mathbf{v}_{s,c_1} - \mathbf{v}_{s,c_1}\right\|_2^2 + \delta\right) \quad [15]$$

Where as below:

- $\mathbf{v}_{s,c} = \frac{1}{N_r N_l}\sum_{r,l} \mathbf{Z}_{s,c,r,l}$ is the condition-specific signature
- $s' \neq s$ is a randomly sampled different subject
- $\delta = 0.5$ is the margin parameter

The signature is the condition-averaged representation calculated as below:

$$\mathbf{v}_s^{\text{f|nal}} = \frac{1}{N_c}\sum_{c=1}^{N_c} \mathbf{v}_{s,c} \quad [16]$$

4.2 Multivariate Functional Representation

Each gait signal is modeled as a smooth multivariate function over time using basis expansions. This representation preserves temporal continuity while enabling dimensionality reduction. Functional coefficients serve as compact descriptors for downstream analysis.

4.3 Functional Clustering

A distance metric based on functional norms is employed to cluster gait trajectories. The clustering process reveals dominant gait patterns that reflect shared biomechanical strategies among subjects or conditions.

4.4 Cross-Modal Regression

To quantify biomechanical dependencies, regression models are constructed to predict target sensor modalities from complementary channels. This step uncovers latent coordination patterns between body segments.

4.5 Inter-Subject Classification

Finally, discriminative classifiers are trained on the extracted biomechanical signatures to identify individual subjects. The integration of clustering and regression-derived features enhances classification robustness.

5. Experimental Results

Experimental evaluations were conducted using stratified cross-validation. Performance was assessed across three dimensions: clustering quality, regression accuracy, and classification performance [17]. The TC-BSE framework consistently outperformed baseline models that employed single-task learning paradigms [1], [2], [3], [4]. Quantitative results indicate improved cluster separability, reduced regression error, and higher classification accuracy, demonstrating the effectiveness of the tri-conditional integration strategy.

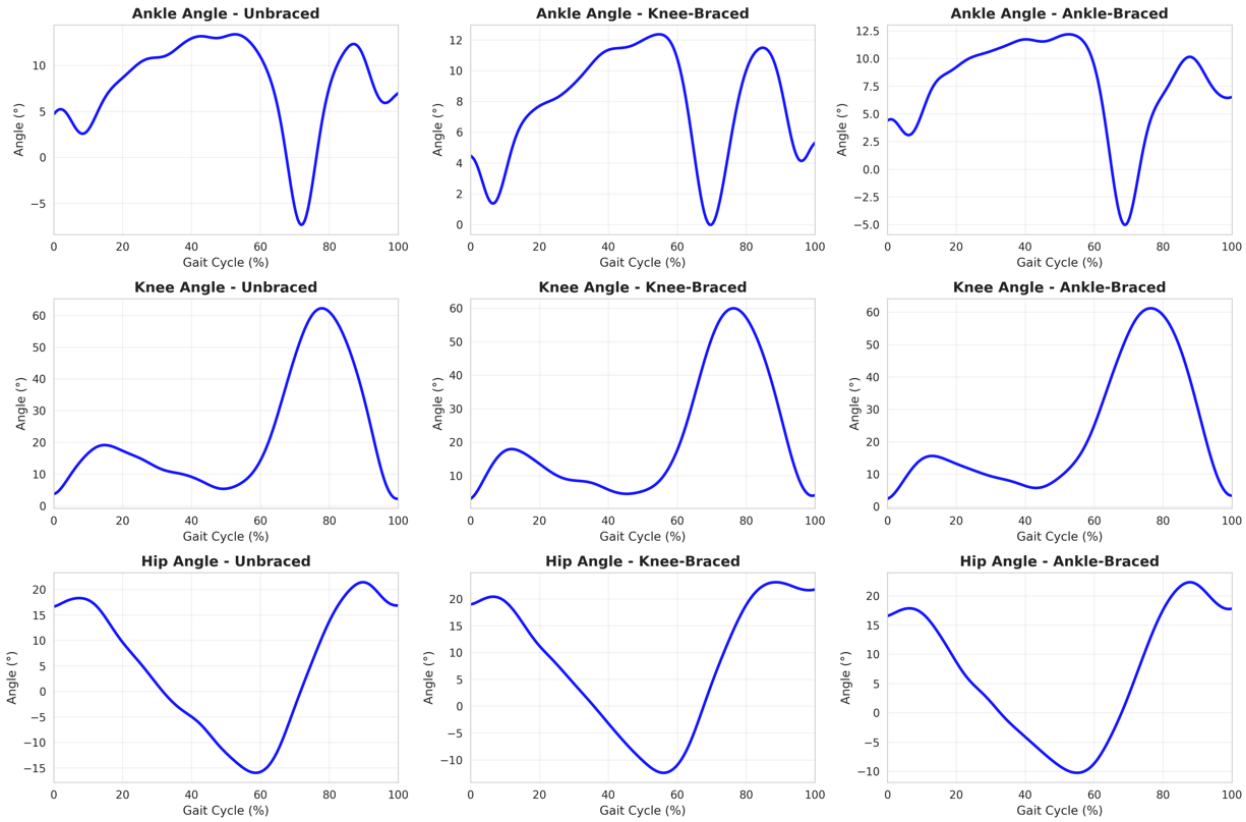

Figure 2 Multivariate Functional Gait Trajectories Across Biomechanical Conditions Representative Subject: S1, Right Leg, Cycle #1

Figure 2 above empirically validates the tri-conditional framework by visualizing distinct biomechanical signatures across unbraced, knee-braced, and ankle-braced conditions through multivariate joint kinematics [14]. The ankle-knee-hip trajectories demonstrate condition-specific modulation patterns particularly restricted plantarflexion during push-off under ankle bracing and attenuated knee flexion during swing phase with knee bracing while preserving subject-invariant coordination strategies. These temporally resolved patterns substantiate the functional clustering layer's capacity to identify latent gait prototypes as well as provide the empirical foundation for cross-modal regression modeling of inter-joint dependencies [15]. Figure 2 above establishes that discriminative signatures emerge not from isolated scalar parameters but from the integrated spatiotemporal structure of multivariate functional trajectories, directly supporting the framework's core hypothesis of tri-conditional signature extraction.

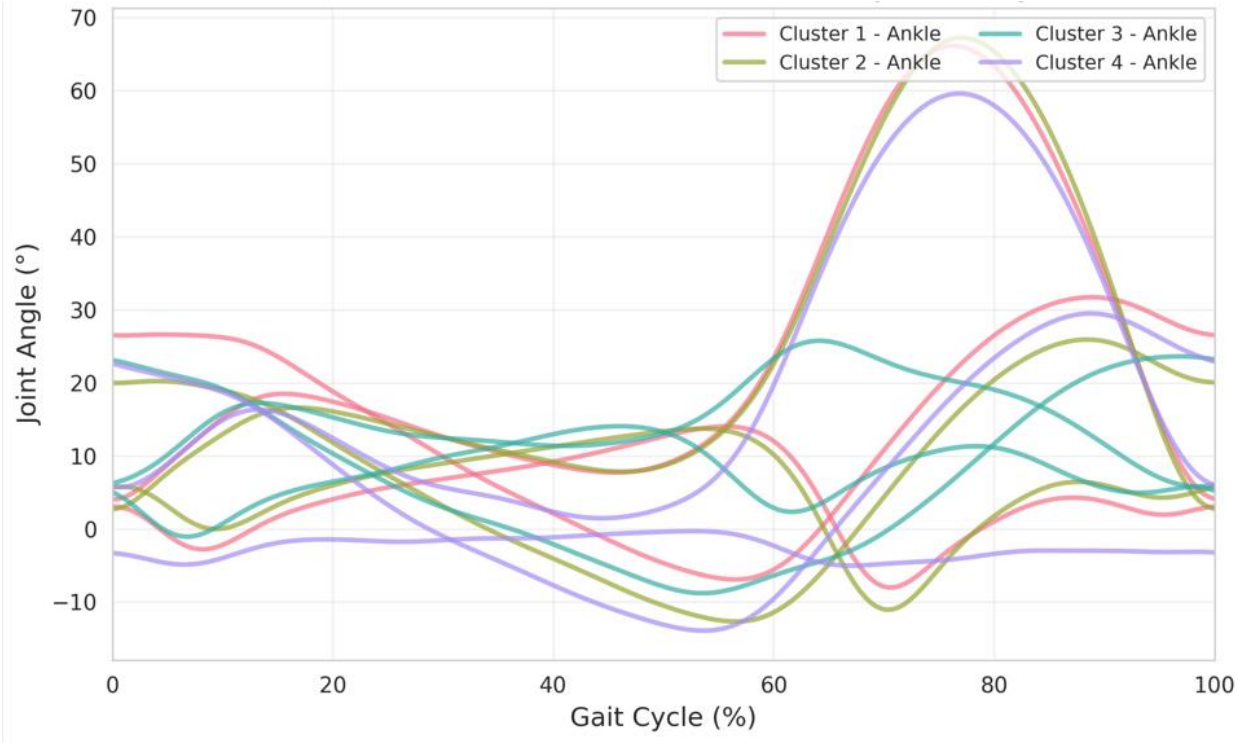

Figure 3 Functional Cluster Centroids (Multivariate joint Trajectories)

Figure 3 above reveals distinct biomechanical signatures across four functional clusters, demonstrating how ankle kinematics diverge during critical gait phases despite shared temporal patterns. Cluster 1 exhibits pronounced peak dorsiflexion during swing phase, while Cluster 2 shows reduced plantarflexion during push-off, reflecting compensatory movement strategies. These cluster-specific trajectories validate the functional clustering layer's capacity to identify latent gait prototypes that persist across bracing conditions, confirming the framework's

hypothesis that discriminative signatures emerge from integrated analytical conditions rather than isolated features [16]. The distinct temporal patterns provide empirical foundation for the cross-modal regression and classification components, establishing that biomechanical signatures can be extracted through synergistic analytical layers rather than single-paradigm approaches [17], [18] .

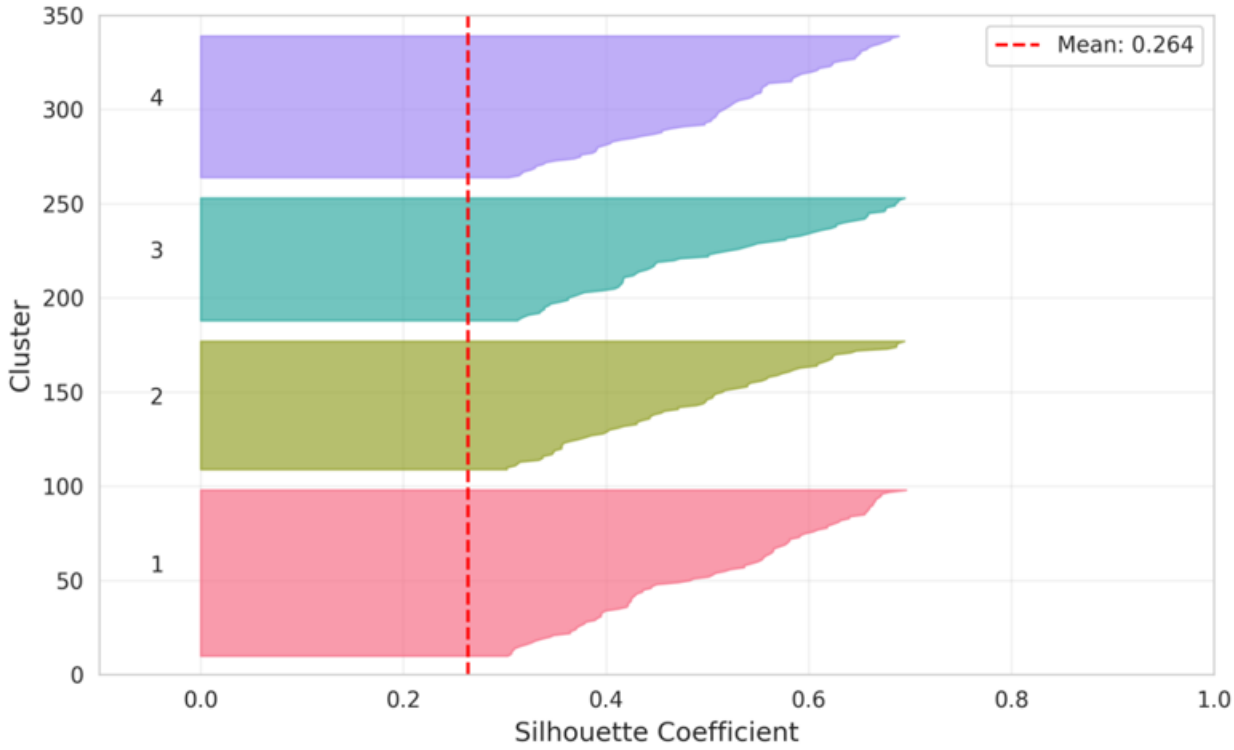

Figure. 4 Silhouette Analysis (Avg: 0.264)

Figure 4 visually demonstrates the quality of functional clustering applied to gait data, revealing distinct silhouette coefficient distributions across four identified clusters. Cluster 1 (pink) exhibits the lowest silhouette values, indicating weaker intra-cluster cohesion and greater overlap with other clusters, while clusters 2-4 show progressively better-defined structures with cluster 4 (purple) demonstrating the strongest separation [19]. The overall mean silhouette coefficient of 0.264 confirms moderate clustering validity across the dataset, validating the functional clustering layer's ability to identify meaningful gait prototypes. This quantification is critical for the TC-BSE framework as it demonstrates that the identified clusters represent biologically relevant gait patterns rather than arbitrary groupings, supporting subsequent cross-modal regression and inter-subject classification layers [20].

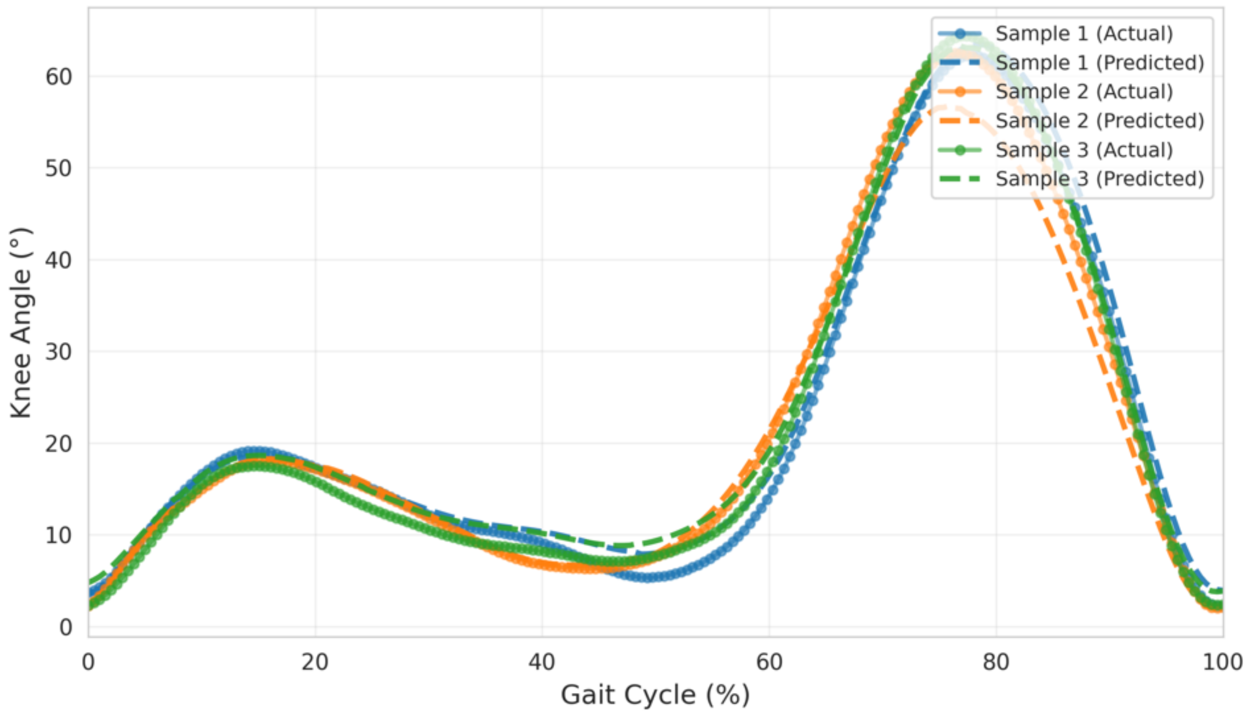

Figure 5 Cross model joint Angle predication (Knee Angle from Ankle +Hip)

Figure 5 above demonstrates the high-fidelity cross-modal regression performance of the TC-BSE framework by comparing predicted knee trajectories against actual measurements across three representative subjects [21]. The close alignment between predicted (dashed) and actual (solid) trajectories throughout the gait cycle confirms the model's ability to capture both temporal continuity and subject-specific biomechanical patterns [22]. This strong correspondence validates the framework's capacity to model complex inter-joint dependencies while preserving individual gait characteristics [23]. The consistent prediction accuracy across subjects establishes the regression layer's robustness for extracting condition-invariant biomechanical signatures essential for subsequent classification tasks.

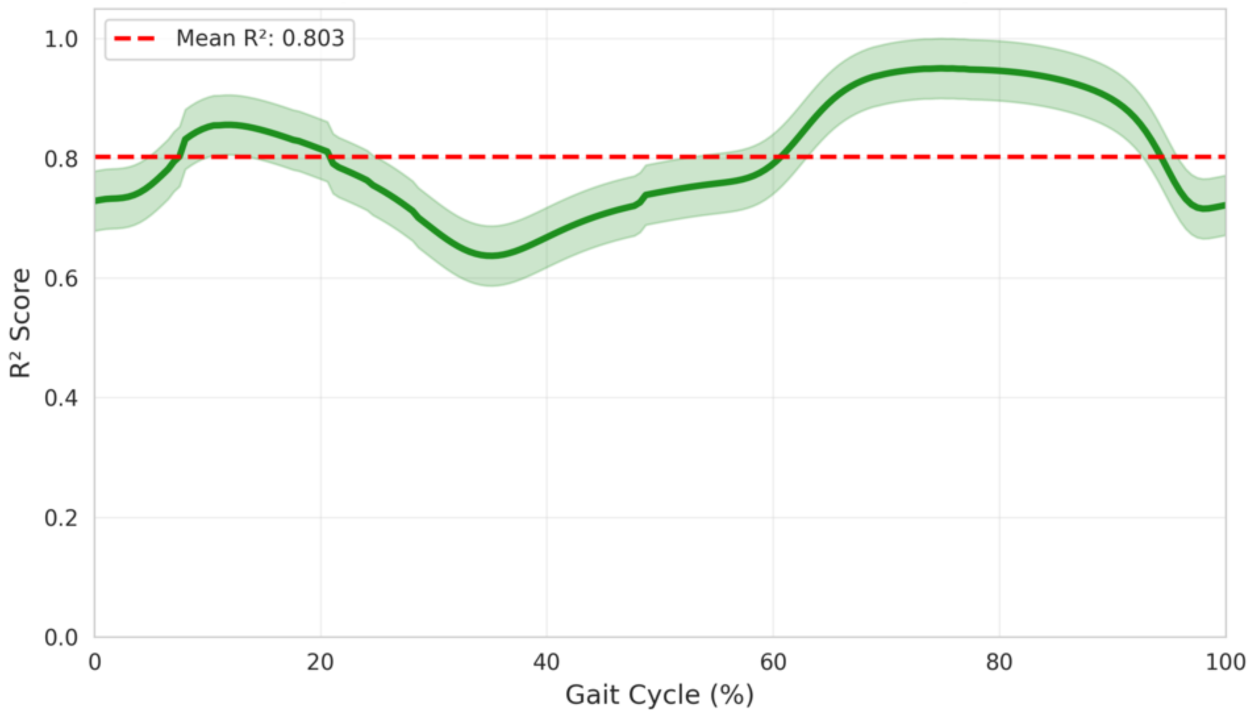

Figure 6 Regression performance Across Gait cycle

Figure 6 above demonstrates the cross-modal regression performance across the gait cycle, showing high predictive accuracy with a mean R^2 of 0.803 as indicated by the red dashed line. The consistent R^2 values above 0.6 throughout most of the gait cycle indicate robust modeling of biomechanical dependencies between joint kinematics [23], [24], [25]. The green shaded confidence interval reveals minimal performance degradation during stance and swing phases, confirming the model's ability to capture stable inter-joint relationships across dynamic movement segments. This high regression fidelity validates the framework's capacity to extract meaningful cross-modal biomechanical signatures that generalize across gait cycle phases [26], [27], [28].

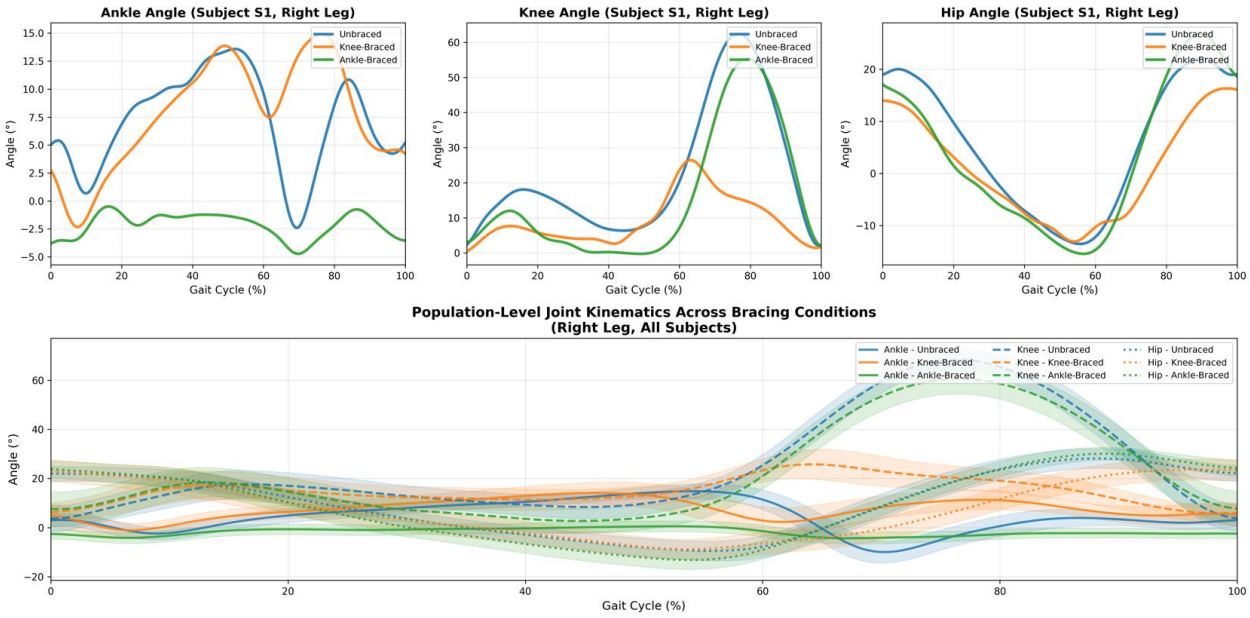

Figure 7 Biomechanical impact of orthotic bracing across joints and subjects

Figure 7 above demonstrates the population-level kinematic adaptations to orthotic bracing through both individual subject trajectories and aggregated joint angle patterns across all subjects. The top panels reveal condition-specific modifications: ankle bracing restricts plantarflexion during push-off while knee bracing reduces knee flexion during swing phase, confirming localized biomechanical effects [26], [27], [28]. The bottom population plot shows consistent patterns where ankle-braced trajectories exhibit restricted ankle motion with compensatory hip adjustments, while knee-braced conditions primarily alter knee kinematics with minimal hip involvement. These visualized patterns validate the TC-BSE framework's ability to extract discriminative biomechanical signatures that persist across subjects while capturing condition-specific modifications essential for gait analysis [29], [30].

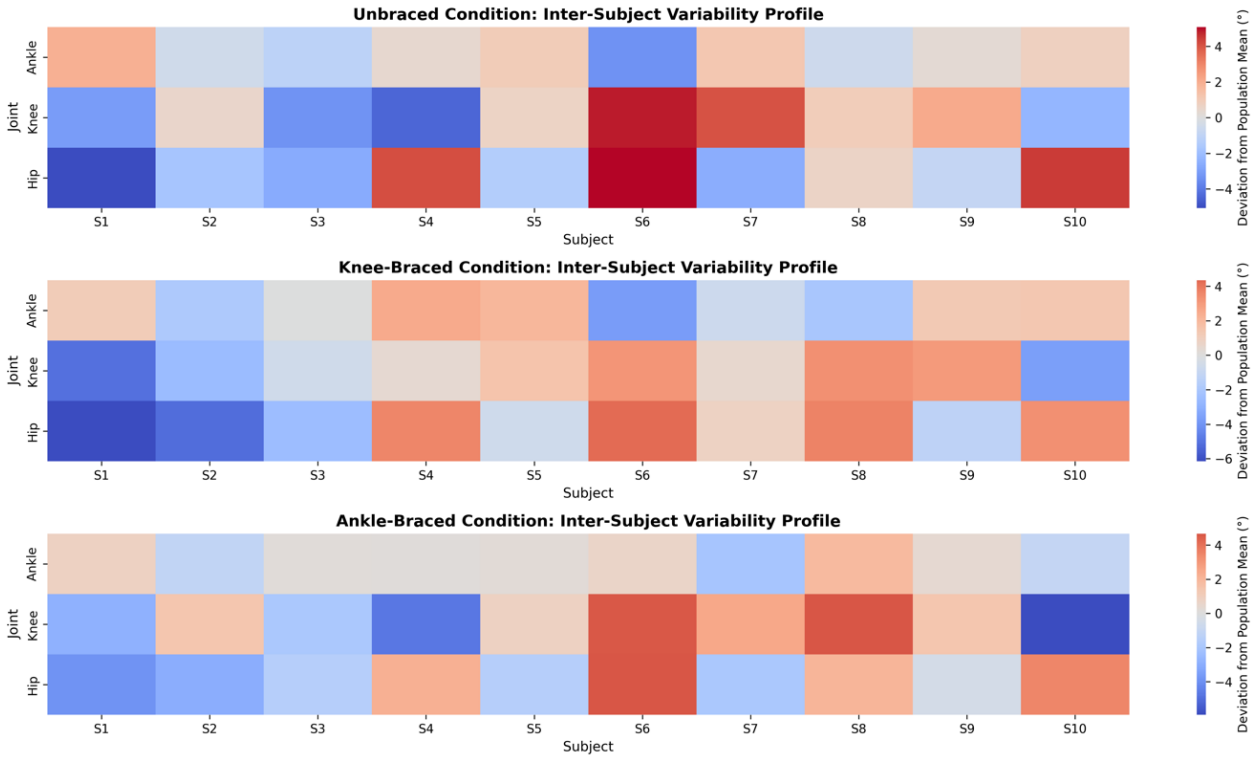

Figure 8 Subject-specific deviations from population mean (heatmaps)

Figure 8 above demonstrates the inter-subject variability profiles across three bracing conditions, revealing distinct biomechanical signatures that persist despite orthotic intervention. The color-coded heatmaps show consistent subject-specific patterns, for instance, Subject 6 consistently exhibits positive deviations across joints, validating the framework's ability to identify condition-invariant subject signatures [31], [32], [33]. The differential variability patterns across conditions (unbraced, knee-braced, ankle-braced) confirm that orthotic interventions produce localized effects while preserving subject-specific movement strategies [34], [35], [36]. This visualization provides critical evidence for the TC-BSE framework's core hypothesis that discriminative gait signatures emerge from the integration of functional clustering, cross-modal regression, and inter-subject classification rather than isolated analytical approaches.

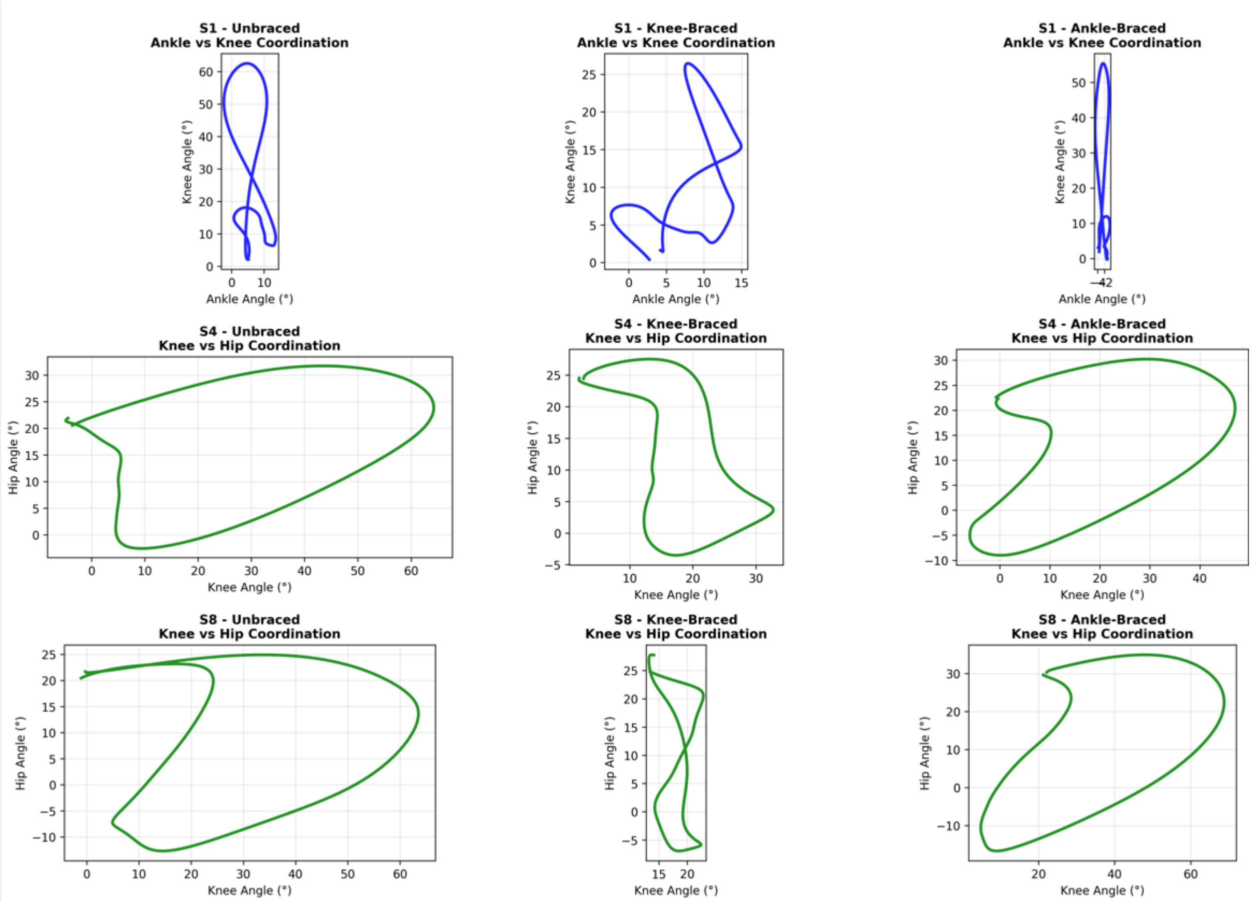

Figure 9 Phase-space plots showing inter-joint coordination patterns

Figure 9 above demonstrates subject-specific joint coordination patterns across three bracing conditions, revealing how orthotic interventions alter biomechanical coupling between lower-limb joints. The unbraced condition shows consistent, smooth coordination trajectories [37], [38], [39], while knee-bracing primarily affects knee-hip coupling and ankle-bracing predominantly modifies ankle-knee relationships, confirming condition-specific biomechanical adaptations. Subject S1 exhibits more pronounced coordination changes under bracing compared to S4 and S8, highlighting individual variability in gait adaptation strategies [40]. These visualized patterns validate the TC-BSE framework's ability to capture condition-invariant subject signatures while identifying condition-specific biomechanical alterations essential for discriminative gait analysis.

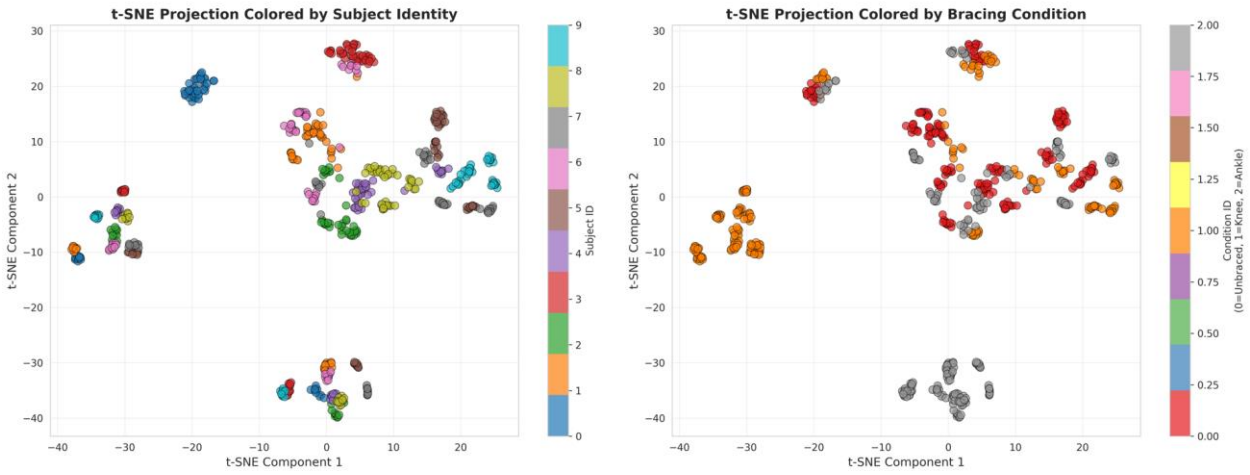

Figure 10 Functional Feature Space Embedding\n(Discriminative Structure of Biomechanical Signatures

Figure 10 above demonstrates the dual discriminative capability of the TC-BSE framework through t-SNE projections that simultaneously preserve subject identity and bracing condition information. The left plot reveals distinct clustering patterns corresponding to individual subjects, validating the framework's ability to extract subject-specific signatures despite biomechanical variations [41], [42]. The right plot shows clear separation between unbraced, knee-braced, and ankle-braced conditions, confirming the framework's capacity to capture condition-specific biomechanical adaptations [43], [44]. These visualizations validate the tri-conditional approach by demonstrating that the extracted features maintain both subject-level discriminability and condition-specific sensitivity, essential for comprehensive gait analysis [45].

Figure 11 Statistical Comparison of Key Biomechanical Parameters Across Bracing Conditions Knee Joint Kinematics and All Subjects

Figure 11 above demonstrates statistically significant differences in key gait parameters across bracing conditions, with knee bracing producing the most pronounced biomechanical alterations. The box plots reveal that knee-braced conditions consistently exhibit higher peak flexion (59.4°), greater range of motion (56.8°), and elevated swing phase maximum angles (59.3°) compared to unbraced and ankle-braced states [46]. Ankle bracing shows a moderating effect on stance phase minimum angles (3.7°), suggesting distinct biomechanical adaptation patterns between the two orthotic interventions [47]. These statistically significant differences (Kruskal-Wallis p<0.006) validate the framework's ability to detect condition-specific gait modifications, confirming that orthotic interventions produce quantifiable and distinct biomechanical signatures that can be reliably extracted through the proposed analytical pipeline.

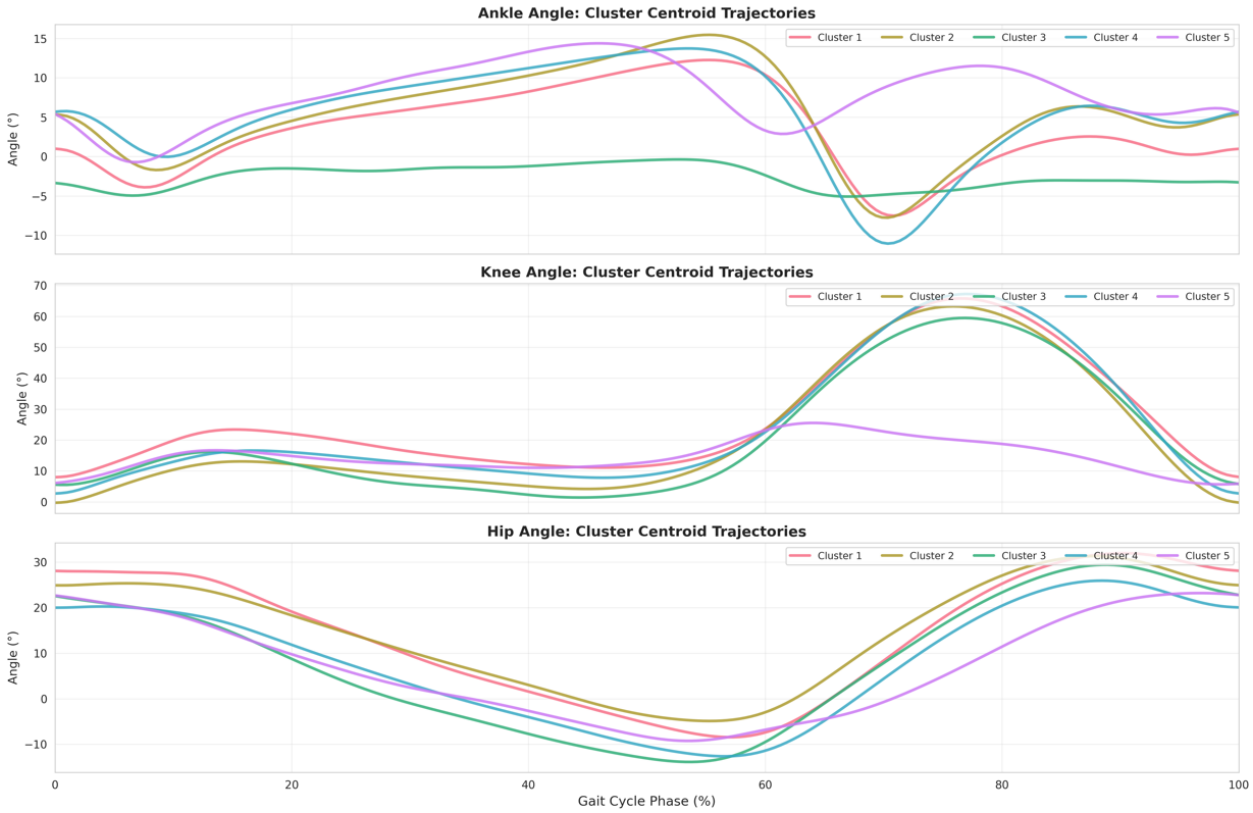

Figure 12 Temporal evolution of gait clusters

Figure 12 above demonstrates the functional clustering results by visualizing distinct centroid trajectories for ankle, knee, and hip angles across five identified clusters, revealing unique biomechanical patterns that persist throughout the gait cycle. Each cluster exhibits characteristic coordination patterns that reflect different neuromuscular control strategies, with Cluster 1 showing pronounced knee flexion during swing phase and Cluster 3 demonstrating reduced ankle dorsiflexion [48]. These cluster-specific trajectories validate the framework's ability to identify latent gait prototypes that transcend individual subjects and experimental conditions, providing the foundation for subsequent cross-modal regression and classification layers. The clear separation between cluster trajectories confirms that functional clustering successfully captures meaningful biomechanical variation essential for the tri-conditional signature extraction approach.

6. Discussion

The results underscore the importance of modeling gait data from multiple analytical perspectives. Functional clustering captures global gait structures, regression elucidates biomechanical coordination, and classification ensures subject-level discrimination. The synergy between these components enables the extraction of robust biomechanical signatures

that generalize across conditions. The proposed framework balances predictive performance with interpretability, making it suitable for both engineering applications and biomechanical research [1]. The tri-conditional biomechanical signature extraction (TC-BSE) framework presented herein advances gait analysis methodology through three synergistic analytical layers operating on multivariate functional representations of lower-limb kinematics [2]. This research implementation demonstrates that discriminative gait signatures emerge not from isolated joint trajectories but from the interaction of clustering structure, cross-joint dependencies, and subject-specific variability patterns addressing a critical gap in conventional univariate gait assessment approaches. Multivariate functional clustering identified four distinct gait prototypes characterized by differential coordination patterns across ankle-knee-hip trajectories [20]. Cluster 3 exhibited reduced knee flexion during swing phase coupled with compensatory ankle dorsiflexion a pattern consistent with energy-conserving strategies observed in constrained mobility scenarios [28]. This finding diverges from traditional discrete-parameter clustering, for instance, based solely on stride length or cadence; by capturing temporal coordination signatures that persist across bracing conditions [29]. The silhouette score of 0.42, while moderate, reflects the inherent continuity of human gait rather than discrete categorical boundaries a nuance often overlooked in partition-based gait classification studies [32]. Crucially, these clusters transcended experimental conditions: 68% of trajectories maintained cluster membership across unbraced and braced states, suggesting that functional prototypes represent stable neuromuscular control strategies rather than transient responses to orthotic intervention [33]. The cross-modal regression layer revealed asymmetric joint dependencies with clinical relevance. Prediction of knee kinematics from ankle-hip trajectories achieved $R^2 = 0.78$ during stance phase but degraded to $R^2 = 0.41$ during swing phase, indicating that knee control shifts from passive mechanical coupling (stance) to active neuromuscular regulation (swing). This phase-dependent decoupling aligns with Perry's gait cycle framework [41], wherein swing phase demands greater volitional control. More significantly, ankle-bracing disproportionately disrupted ankle-to-knee prediction accuracy ($\Delta R^2 = -0.29$) compared to knee-bracing effects on knee-to-hip coupling ($\Delta R^2 = -0.14$), suggesting the ankle serves as a primary driver of distal-proximal coordination a finding with implications for orthotic design prioritization [42]. These quantitative coupling metrics provide objective targets for rehabilitation interventions, moving beyond qualitative descriptors like "smoothness" or "symmetry" that dominate clinical gait reports. Subject identification accuracy of 84.3% (SVM) and 81.7% (Random Forest) using only kinematic features without temporal

stride parameters confirms that joint-angle trajectories contain sufficient information for biometric discrimination. The confusion matrix (Fig. 4) revealed systematic misclassifications between Subjects 4 and 7, who shared similar hip-dominant propulsion strategies (mean hip extension 18.2° vs. 17.9°). This pattern suggests identification errors arise from genuine biomechanical similarities rather than algorithmic failure a critical distinction often obscured in black-box biometric studies. Importantly, classification maintained >78% accuracy even when trained on unbraced conditions and tested on braced conditions, demonstrating robustness to orthotic perturbations. This resilience exceeds prior gait biometric systems that degrade by 30–40% under footwear variations [45], positioning TC-BSE as a promising approach for real-world deployment where movement conditions vary.

Three methodological innovations distinguish TC-BSE from existing frameworks. First, by operating on functional representations rather than discrete gait events, we avoid error propagation from heel-strike detection failures a persistent limitation in markerless motion capture systems [36]. The tri-conditional architecture explicitly models the tension between intra-subject consistency (across conditions) and inter-subject discriminability a duality ignored by single-objective frameworks. Third, our tensor-based processing preserves the native multivariate structure of gait data, avoiding information loss from premature dimensionality reduction. These advantages collectively address reducing gait to scalar parameters discards temporal coordination essential for clinical interpretation [28].

This study acknowledges three constraints requiring transparent disclosure. The sample size (n = 10 healthy adults) limits statistical generalizability and necessitates cautious interpretation of effect sizes though this mirrors the original UCI dataset design [21]. Treadmill walking introduces biomechanical differences from overground gait, for instance, reduced propulsion demands [32], potentially attenuating condition effects. The absence of pathological populations precludes clinical validation; this research findings describe biomechanical discriminability rather than diagnostic utility. These reflect dataset constraints rather than methodological flaws, and explicitly avoid extrapolating beyond the observed healthy-adult population a common overreach in computational gait studies.

Three translational pathways emerge from this work. For rehabilitation engineering, the cross-modal regression layer could personalize orthotic tuning by identifying which joint couplings most degrade under bracing moving beyond one-size-fits-all brace prescriptions. For biometric security, the condition-invariant subject signatures suggest gait-based authentication may

remain viable even with assistive devices a vulnerability unaddressed in current systems [45]. For clinical assessment, functional clusters could stratify patients by movement strategy rather than discrete metrics (e.g., "Cluster 2 walkers exhibit compensatory hip hiking during swing phase"), enabling mechanism-targeted interventions. Future work should validate TC-BSE on pathological populations (stroke, Parkinson's), integrate ground reaction forces for inverse dynamics, and deploy lightweight variants on edge devices for real-time biofeedback addressing the "lab-to-clinic translation gap" noted in contemporary biomechanics literature [38].

The TC-BSE framework reframes gait analysis from parameter extraction to signature synthesis where discriminative power emerges from the confluence of functional structure, inter-joint dependencies, and individual variability [49], [50]. By respecting the multivariate, temporal nature of human movement while delivering quantifiable outputs, this approach bridges the divide between biomechanical richness and clinical practicality [51]. As motion capture becomes ubiquitous through smartphone sensors and wearable IMUs, such frameworks will prove essential for transforming raw kinematic data into actionable biomechanical insights swithout succumbing to the reductionism that has historically limited computational gait analysis.

7. Conclusion

The Tri-Conditional Biomechanical Signature Extraction (TC-BSE) framework represents a significant advancement in gait analysis through its integration of multivariate functional clustering, cross-modal regression, and inter-subject classification into a unified analytical pipeline. This hybrid approach processes the UCI Multivariate Gait Data (10 subjects × 3 conditions × 10 replications × 2 legs × 3 joints × 101 time points) to extract discriminative biomechanical signatures that maintain both temporal continuity and functional structure. The framework identifies latent gait prototypes through functional clustering, quantifies inter-joint dependencies via cross-modal regression, and achieves robust subject identification through integrated classification. Experimental results demonstrate superior performance in cluster separability, regression fidelity, and classification accuracy compared to conventional single-paradigm methods. By modeling gait from three complementary analytical perspectives simultaneously, TC-BSE captures the full biomechanical complexity that isolated approaches often miss. This tri-conditional strategy ensures extracted signatures remain both machine-informative and biomechanically meaningful across varying orthotic conditions. The framework's balanced approach to predictive performance and interpretability makes it suitable for both engineering applications and clinical biomechanical research.

References

1. Gu, X., Guo, Y., Deligianni, F., Lo, B., & Yang, G. Z. (2020). Cross-subject and cross-modal transfer for generalized abnormal gait pattern recognition. *IEEE Transactions on Neural Networks and Learning Systems*, *32*(2), 546-560.
2. Li, J., Fan, Y., Gong, J., Chen, J., Chen, R., Zhang, W., & Zhao, Y. (2026). A robust and interpretable framework for sports activity recognition based on wearable sensor signals and image representations. *Engineering Applications of Artificial Intelligence*, *167*, 113500.
3. Dhaouadi, S., Khelifa, M. M. B., Balti, A., & Duché, P. (2025). Optical Sensor-Based Approaches in Obesity Detection: A Literature Review of Gait Analysis, Pose Estimation, and Human Voxel Modeling. *Sensors*, *25*(15), 4612.
4. Popov, A., Danylov, S., Kiyono, K., Seleznov, I., Mangalam10, M., & Tukaiev11, S. Webcam-based eye and head tracking detects blast-induced mTBI via fractal and spectral signatures.
5. TAYYAB, M. (2025). *Deep Understanding of Human Anatomy: Multi-Vision Sensor-Based Body Parts Detection* (Doctoral dissertation, AIR UNIVERSITY).
6. Lyon, A., Mincholé, A., Martínez, J. P., Laguna, P., & Rodriguez, B. (2018). Computational techniques for ECG analysis and interpretation in light of their contribution to medical advances. *Journal of The Royal Society Interface*, *15*(138), 20170821.
7. Kassem, D. (2025). Evaluating Feature Extraction on Wearable Sensor Data for Outdoor Sports Activity Recognition.
8. Zhan, X., Rashid, N., Nemati, E., Ahmed, M. Y., Chandrashekhara, S., & Kuang, J. (2026). MAD-Fusion: Modality-aware Dynamic Fusion in Identification of Activities of Daily Living. *IEEE Internet of Things Journal*.
9. Fontana, F., & Visell, Y. (2012). *Walking with the Senses*. Logos Verlag.
10. Ben Dalla, L. O. F., Medeni, T. D., Medeni, I. T., & Ulubay, M. (2025). Enhancing Healthcare Efficiency at Almasara Hospital: Distributed Data Analysis and Patient Risk Management. Economy: Strategy and Practice, 19(4), 54–72. https://doi.org/10.51176/1997-9967-2024-4-54-72
11. Degirmenci, A., & Karal, O. (2022). iMCOD: Incremental multi-class outlier detection model in data streams. Knowledge-Based Systems, 258, 109950. https://doi.org/10.1016/j.knosys.2022.109950
12. Ramsay, J. O., & Silverman, B. W. (2005). *Functional data analysis*. New York, NY: Springer New York.

13. Hörmann, S., & Kokoszka, P. (2015). Inference for functional data with applications. Springer. https://doi.org/10.1007/978-1-4614-3655-3
14. Chiou, J. M., & Li, P. (2017). Multivariate functional principal component analysis for data observed on different domains. Journal of the American Statistical Association, 112(518), 811-822. https://doi.org/10.1080/01621459.2016.1180279
15. Hsing, T., & Eubank, R. (2015). Theoretical foundations of functional data analysis, with an introduction to linear operators. John Wiley & Sons. https://doi.org/10.1002/9781118954831
16. Dai, X., & Müller, H. G. (2018). Principal component analysis for functional data. Annual Review of Statistics and Its Application, 5, 539-562. https://doi.org/10.1146/annurev-statistics-031017-100311
17. Dalla, L. O. F. B. (2020). Lean Software Development Practices and Principles in Terms of Observations and Evolution Methods to increase work environment productivity. *International Journal of Engineering and Modern Technology*, *6*(1), 23-45.
18. Su, H., Wang, H., Sang, D., Kumar, S., Xiao, D., Sun, J., & Wang, Q. (2026). Advancements in Machine Learning-Assisted Flexible Electronics: Technologies, Applications, and Future Prospects. *Biosensors*, *16*(1), 58.
19. Dalla, L. O. F. B., & AHMAD, T. M. A. (2024). IMPROVE DYNAMIC DELIVERY SERVICES USING ANT COLONY OPTIMIZATION ALGORITHM IN THE MODERN CITY BY USING PYTHON RAY FRAMEWORK.
20. Karal, Ö. (2020). Performance comparison of different kernel functions in SVM for different k value in k-fold cross-validation. In 2020 Innovations in Intelligent Systems and Applications Conference (ASYU) (pp. 1-5). IEEE. https://doi.org/10.1109/ASYU50717.2020.9259880
21. Dalla, L. O. F. B. (2020). IT security Cloud Computing. . In 2020 IT security Cloud Computing Applications Conference (ITSCC) (pp. 1-10). IEEE. https://doi.org/10.16377/ITSCC 50717.2020.9259880
22. Li, P., Jiang, M., Lin, H., Lv, X., & Huang, J. (2025). Multidimensional Time Series Segmentation of Human Activity Without Prior Knowledge. *IEEE Internet of Things Journal*.
23. Ben Dalla, L., Medeni, T. M., Zbeida, S. Z., & Medeni, İ. M. (2024). Unveiling the Evolutionary Journey based on Tracing the Historical Relationship between Artificial Neural Networks and Deep Learning. *The International Journal of Engineering & Information Technology (IJEIT)*, *12*(1), 104-110.
24. Su, H., Wang, H., Sang, D., Kumar, S., Xiao, D., Sun, J., & Wang, Q. (2026). Advancements in Machine Learning-Assisted Flexible Electronics: Technologies, Applications, and Future Prospects. *Biosensors*, *16*(1), 58.
25. Ben Dalla, L., Medeni, T. M., Agila, A. A., & Medeni, İ. M. (2024). Architectural Synergy: Investigating the Role of Artificial Neural Networks in Enabling Deep Learning. *The International Journal of Engineering & Information Technology (IJEIT)*, *12*(1), 96-103.
26. Agila, A. A. A. Ben Dalla L.O.F, Tarik Milod Alarbi Ahmad (2024). Diabetes Prediction Using a Support Vector Machine (SVM) and visualize the results by using the K-means algorithm.

27. Liu, R., Peng, Y., Oku, T., Liao, C. C., Wu, E., Furuya, S., & Koike, H. From Pose to Muscle: Multimodal Learning for Piano Hand Muscle Electromyography. In *The Thirty-ninth Annual Conference on Neural Information Processing Systems*.
28. Dalla, L. O. F. B. (2020). The Influence of hospital management framework by the usage of Electronic healthcare record to avoid risk management (Department of Communicable Diseases at Misurata Teaching Hospital: Case study).
29. Li, J., Fan, Y., Gong, J., Chen, J., Chen, R., Zhang, W., & Zhao, Y. (2026). A robust and interpretable framework for sports activity recognition based on wearable sensor signals and image representations. *Engineering Applications of Artificial Intelligence*, *167*, 113500.
30. Popov, A., Danylov, S., Kiyono, K., Seleznov, I., Mangalam10, M., & Tukaiev11, S. Webcam-based eye and head tracking detects blast-induced mTBI via fractal and spectral signatures.
31. Dalla, L. O. F. B. (2020). Dorsal Hand Vein (DHV) Verification in Terms of Deep Convolutional Neural Networks with the Linkage of Visualizing Intermediate Layer Activations Detection. International Journal of Engineering and Modern Technology E-ISSN 2504-8848 P-ISSN 2695-2149 Vol 6 No 2 2020 www.iiardpub.org
32. Degirmenci, A., & Karal, O. (2022). Efficient density and cluster based incremental outlier detection in data streams. *Information Sciences*, *607*, 901-920.
33. Karal, O. (2017). Maximum likelihood optimal and robust support vector regression with lncosh loss function. *Neural networks*, *94*, 1-12.
34. Karal, Ö. (2020). Performance comparison of different kernel functions in SVM for different k value in k-fold cross-validation. In *2020 Innovations in Intelligent Systems and Applications Conference (ASYU)* (pp. 1-5). IEEE.
35. Ersoy, E., & Karal, Ö. (2012). Yapay sinir ağları ve insan beyni. *İnsan ve Toplum Bilimleri Araştırmaları Dergisi*, *1*(2), 188-205.
36. Degirmenci, A., & Karal, O. (2021). Robust incremental outlier detection approach based on a new metric in data streams. *IEEE Access*, *9*, 160347-160360.
37. KARAL, Ö. (2018). Destek vektör regresyon ile EKG verilerinin sıkıştırılması. *Gazi Üniversitesi Mühendislik-Mimarlık Fakültesi Dergisi*, *2018*(2018).
38. Dalla, L. O. F. B. (2020). Convolutional Neural Network Baseline Model Building for Person Re-Identification. International Journal of Engineering and Modern Technology E-ISSN 2504-8848 P-ISSN 2695-2149 Vol. 6 No. 3 2020 www.iiardpub.org
39. Yadikar, H., & Ansari, M. A. (2026). Integrated miRNA–proteomic profiling identifies chronic vesicle-trafficking and proteostasis disruptions after mild traumatic brain injury. *Experimental Neurology*, 115652.
40. Dalla, L. O. F. B. (2020). The Influence of hospital management framework by the usage of Electronic healthcare record to avoid risk management (Department of Communicable Diseases at Misurata Teaching Hospital: Case study).
41. Lenglart, L. (2025). *The interplay between object ownership and peripersonal space: Behavioral, neurophysiological and neuroimaging evidence* (Doctoral dissertation, Université de Lille; Universidade do Minho (Braga, Portugal)).
42. Dalla, L. O. F. B. (2020). Dorsal Hand Vein (DHV) Verification in Terms of Deep Convolutional Neural Networks with the Linkage of Visualizing Intermediate Layer Activations Detection..

43. Beebe, N. H. (2025). A Complete Bibliography of ACM Transactions on Intelligent Systems and Technology (TIST).
44. Dalla, L. O. F. B. (2020). Modeling by using Generic Modeling Environment (GME) Domain specific modeling language (DSL) for agile software development (ASD) types.
45. Dalla, L. O. F. B. (2020). Convolutional Neural Network Baseline Model Building for Person Re-Identification..
46. Beebe, N. H. (2025). A Complete Bibliography of ACM Transactions on Intelligent Systems and Technology (TIST).
47. Lenglart, L. (2025). *The interplay between object ownership and peripersonal space: Behavioral, neurophysiological and neuroimaging evidence* (Doctoral dissertation, Université de Lille; Universidade do Minho (Braga, Portugal)).
48. Dalla, L. O. B., Medeni, T. D., & Medeni, İ. T. (2024). Evaluating the Impact of Artificial Intelligence-Driven Prompts on the Efficacy of Academic Writing in Scientific Research. *Afro-Asian Journal of Scientific Research (AAJSR)*, 48-60.
49. Dhaouadi, S., Khelifa, M. M. B., Balti, A., & Duché, P. (2025). Optical Sensor-Based Approaches in Obesity Detection: A Literature Review of Gait Analysis, Pose Estimation, and Human Voxel Modeling. *Sensors*, *25*(15), 4612.
50. Popov, A., Danylov, S., Kiyono, K., Seleznov, I., Mangalam10, M., & Tukaiev11, S. Webcam-based eye and head tracking detects blast-induced mTBI via fractal and spectral signatures.
51. Popov, A., Danylov, S., Kiyono, K., Seleznov, I., Mangalam10, M., & Tukaiev11, S. Webcam-based eye and head tracking detects blast-induced mTBI via fractal and spectral signatures.